Platinum(II) and Palladium(II) Complexes of Bisphosphine Ligands Bearing *o-N,N*-Dimethylanilinyl Substituents: A Hint of Catalytic Olefin Hydration

Nathan D. Jones,[†] Patric Meessen, Udo Losehand, Brian O. Patrick, and Brian R. James*

Department of Chemistry, University of British Columbia, Vancouver, Canada V6T 1Z1

Platinum(II) and palladium(II) complexes of the potentially hexadentate *P,N*-donor ligand family Ar_2P-X-PAr_2 (X = $(CH_2)_2$ [dmape], *cyclic*-C_5H_8 [dmapcp]; Ar = *o-N,N*-dimethylanilinyl) are described. In CH_2Cl_2, the dmape complexes exist as equilibrium mixtures of $MCl_2(P,P'$-dmape) and [MCl(P,P',N-dmape)]Cl isomers (M = Pd, Pt), governed by $\Delta H° = -19 \pm 4$ kJ mol^{-1} and $\Delta S° = -100 \pm 30$ J mol^{-1} K^{-1} for M = Pt, and $\Delta H° = -11 \pm 7$ kJ mol^{-1} and $\Delta S° = -60 \pm 20$ J mol^{-1} K^{-1} for M = Pd. The water-soluble dmapcp complexes exist solely in the [MCl(P,P',N-dmapcp)]Cl form, but the free and coordinated anilinyl rings in these complexes are in slow diastereoselective exchange. X-ray crystal structures for $MCl_2(P,P'$-dmape) (M = Pd, Pt), and the [PdCl(P,P',N-dmape)]$^+$ and [PtCl-(P,P',N-dmapcp)]$^+$ cations, are presented. Some of the complexes show marginal activity in water for the catalyzed hydration of maleic to malic acid, giving about 6–7% conversion in 24 h at 100 °C and substrate:catalyst loadings of 100:1. Attempts to synthesize a PdCl(P,P',N-dmapm)$^+$ species led instead to isolation of [Pd(μ-Cl)(P,P'-dmapm)]$_2$-[PF_6]$_2$ (dmapm = $Ar_2PCH_2Ar_2$).

Introduction

Work in our laboratories over the last 15 years has pursued the use of *o*-pyridyl-substituted[1–6] and *o*-anilinyl-substituted[7–11] mono-[1–4,7] and bis(phosphine)[4–6,8–11] ligands in platinum group metal chemistry, one of the goals being to find water-soluble transition metal catalysts for olefin hydration.[1–3] More generally, there is a vast literature on complexes of P–N ligands; they are attractive as homogeneous catalysts because their "hard–soft" and hemilabile character permits coordination to a variety of metals in a range of oxidation states,[12–15] and because the presence of N-atoms provides strategies for water-solubilization.[16–19]

Recently, we reported the synthesis and characterization of a family of bis(phosphine) ligands bearing two *o-N,N*-dimethylanilinyl substituents at each P atom: 1,1-bis(di(*o-N,N*-dimethylanilinyl)phosphino)methane (dmapm), 1,2-bis-(di(*o-N,N*-dimethylanilinyl)phosphino)ethane (dmape), and *rac*-1,2-bis(di(*o-N,N*-dimethylanilinyl)phosphino)cyclopentane (dmapcp), illustrated in Chart 1.[8] Horner and Simons[20] reported in 1984 ligands akin to dmape but

* To whom correspondence should be addressed. E-mail: brj@chem.ubc.ca.

† Current address: Department of Chemistry, University of Western Ontario, London, Ontario, Canada N6A 5B7.

(1) Xie, Y.; James, B. R. *J. Organomet. Chem.* **1991**, *417*, 277.
(2) Xie, Y.; Lee, C.-L.; Yang, Y.; Rettig, S. J.; James, B. R. *Can. J. Chem.* **1992**, *70*, 751.
(3) Xie, L. Y.; James, B. R. *Inorg. Chim. Acta* **1994**, *217*, 209.
(4) Baird, I. R.; Smith, M. B.; James, B. R. *Inorg. Chim. Acta* **1995**, *235*, 291.
(5) Jones, N. D.; Rettig, S. J.; James, B. R. *J. Cluster Sci.* **1998**, *9*, 243.
(6) Jones, N. D.; MacFarlane, K. S.; Smith, M. B.; Schutte, R. P.; Rettig, S. J.; James, B. R. *Inorg. Chem.* **1999**, *38*, 3956.
(7) Mudalige, D. C.; Ma, E. S.; Rettig, S. J.; James, B. R.; Cullen, W. R. *Inorg. Chem.* **1997**, *36*, 5426.
(8) Jones, N. D.; Meessen, P.; Smith, M. B.; Losehand, U.; Rettig, S. J.; Patrick, B. O.; James, B. R. *Can. J. Chem.* **2002**, *80*, 1600.
(9) Jones, N. D.; James, B. R. *Adv. Synth. Catal.* **2002**, *344*, 1126.
(10) Jones, N. D.; Foo, S. J. L.; Patrick, B. O.; James, B. R. *Inorg. Chem.* **2004**, *43*, 4056.
(11) Foo, S. J. L.; Jones, N. D.; Patrick, B. O.; James, B. R. *Chem. Commun.* **2003**, 988.

(12) Guiry, P. J.; Saunders: C. P. *Adv. Synth. Catal.* **2004**, *346*, 497.
(13) Fache, F.; Schulz, E.; Tommasino, M. L.; Lemaire, M. *Chem. Rev.* **2000**, *100*, 2159. Newkome, G. R. *Chem. Rev.* **1993**, *93*, 2067.
(14) Espinet, P.; Soulantica, K. *Coord. Chem. Rev.* **1999**, *193–195*, 499.
(15) Braunstein, P.; Naud, F. *Angew. Chem., Int. Ed.* **2001**, *40*, 680. Braunstein, P. *J. Organomet. Chem.* **2004**, *689*, 3953.
(16) Nagel, U.; Kinzel, E. *Chem. Ber.* **1986**, *119*, 1731.
(17) Tóth, I.; Hanson, B. E. *Tetrahedron: Asymmetry* **1990**, *1*, 895. Tóth, I.; Hanson, B. E. *Tetrahedron: Asymmetry* **1990**, *1*, 913. Tóth, I.; Hanson, B. E.; Davis, M. E. *J. Organomet. Chem.* **1990**, *396*, 363. Tóth, I.; Hanson, B. E.; Davis, M. E. *Catal. Lett.* **1990**, *5*, 183.
(18) Lamouille, T.; Saluzzo, C.; ter Halle, R.; Guyader, F. L.; Lemaire, M. *Tetrahedron Lett.* **2001**, *42*, 663.
(19) Nuzzo, R. G.; Feitler, D.; Whitesides, G. M. *J. Am. Chem. Soc.* **1979**, *101*, 3683.

Chart 1. Bisphosphine Ligands Bearing Two *o-N,N*-Dimethylanilinyl Substituents at Each P-Atom
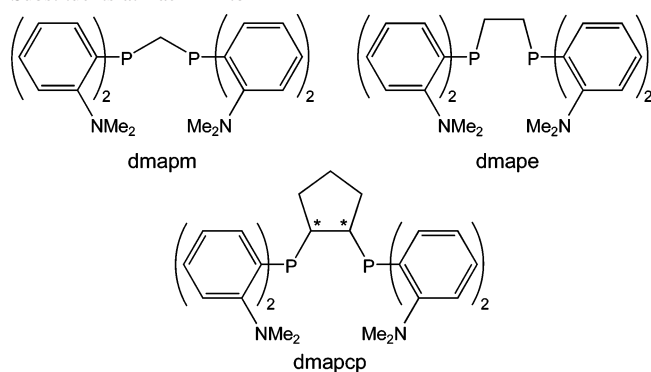
containing only one *o*-substituted NR$_2$ group at each P-atom that was thus chiral; they subsequently used Rh complexes of such ligands as precursors for asymmetric hydrogenation of olefinic substrates.[20] Tóth and co-workers[17] have made related ligands bearing *p*-C$_6$H$_4$(NMe$_2$) substituents, including chiral derivatives with quaternized N-atoms for use in catalytic asymmetric hydrogenation in water; with these systems, simultaneous coordination to the same metal center by the P- and N-atoms of the same ligand is not possible, and there are no reports of bridging by these *p*-substituted ligands. Our *o*-substituted ligands make the N-atoms available for coordination to the same metal as the P atoms, in some cases generating water-soluble complexes (salts) by displacement of halide from the metal coordination sphere.

This article builds upon our earlier reports of homo- and heterobimetallic Pt and Pd complexes supported by a *P,P′*-bridging, bis(*P,N*)-chelating coordination mode of dmapm.[9-11] Here, we describe the synthesis and solution- and solid-state characterization of monometallic Pt^{II} and Pd^{II} complexes of the ligands shown in Chart 1. Details on solution fluxionality, including thermodynamic parameters and stereochemical considerations, are presented, as well as preliminary data on the use of water-soluble species as precursors for the catalytic hydration of the activated olefin, maleic acid, *cis*-CH-(CO$_2$H)=CH(CO$_2$H); activated olefins have become standard substrates for assays of catalytic hydration in water.[1,21-23]

Experimental Section

General. Unless otherwise noted, synthetic procedures were performed using standard Schlenk techniques under dry Ar or N$_2$. The ligands[8] dmapm, dmape, *rac*-dmapcp (see the Introduction, Chart 1), and the precursors PtCl$_2$(cod),[24] *trans*-PdCl$_2$(PhCN)$_2$,[25] and PdCl$_2$(dmapm) (**1**)[10] were made according to literature procedures. All other reagents were purchased from commercial sources and used as supplied. Solvents were dried over the appropriate

(20) Horner, L.; Simons, G. *Phosphorus, Sulfur Relat. Elem.* **1984**, *19*, 65; Z. *Naturforsch. B: Chem. Sci.* **1984**, *39B*, 512.
(21) Bzhasso, N. A.; Pyatnitskii, M. P. Zh. Prikl. Zhim. **1969**, 42, 1610 (through Chem. Abstr. *71*, 101239f). Xie, Y. Ph.D. Thesis, University of British Columbia, Vancouver, 1990. Bennett, M. A.; Jin, H.; Lin, S.; Redina, L. M.; Willis, A. *J. Am. Chem. Soc.* **1995**, *117*, 8335.
(22) Stewart, I. C.; Bergman, R. G.; Toste, F. D. *J. Am. Chem. Soc.* **2003**, *125*, 8696.
(23) Ganguly, S.; Roundhill, D. M. *Organometallics* **1993**, *12*, 4825.
(24) McDermott, J. X.; White, J. F.; Whitesides, G. M. *J. Am. Chem. Soc.* **1976**, *98*, 6521.
(25) Hartley, F. R. *Organomet. Rev. (A)* **1976**, *6*, 119.

agents and distilled under N$_2$ prior to use. Details on the measurements of the NMR spectra, studied in CDCl$_3$ at 300 K, unless specified otherwise (s = singlet, d = doublet, t = triplet, spt = septet, m = multiplet, br = broad, p = pseudo; *J*-values in Hz), the UV−vis spectra (reported as λ$_{max}$ (± 2 nm) [ϵ (M^{-1} cm^{-1})]), the conductivity data at 25 °C for 1 mM solutions (Λ$_M$ in Ω^{1-} mol^{-1} cm^2), and the elemental analyses have been reported recently.[10] IR spectra (KBr disks) were recorded from 500 to 4000 cm^{-1} on a Bomem-Michelson MB-100 FTIR spectrometer, data being reported in cm^{-1}.

Syntheses. [PtCl(*P,P′,N*-dmapcp)]Cl·H$_2$O, 2·H$_2$O. This compound was made from either PtCl$_2$ (via *cis*-PtCl$_2$(MeCN)$_2$) or PtCl$_2$-(cod). **(a) From PtCl$_2$.** To a Schlenk tube containing PtCl$_2$ (100 mg, 0.38 mmol) was added CH$_3$CN (10 mL), and the slurry was refluxed for 2 h to give a yellow solution. The dmapcp ligand (230 mg, 0.38 mmol) was then added to the hot solution that became colorless. The solvent was removed in vacuo and the residue was redissolved in minimum CH$_2$Cl$_2$. Addition of Et$_2$O (20 mL) gave a white powder that was isolated by filtration, washed with Et$_2$O and dried in vacuo at 78 °C. Yield: 240 mg (71%). **(b) From PtCl$_2$-(cod).** To a Schlenk tube charged with PtCl$_2$(cod) (97 mg, 0.26 mmol) and dmapcp (160 mg, 0.26 mmol) was added 1,2-dichloroethane (15 mL), and the resulting colorless solution was refluxed for 17 h. The workup was the same as in method (a). Yield: 150 mg (65%). Anal. Calcd for C$_{37}$H$_{48}$N$_4$Cl$_2$P$_2$Pt·H$_2$O: C 49.7; H 5.6; N 6.3; Found: C 50.0; H 5.7; N 6.1. ^{1}H{^{31}P} NMR: δ 1.32 (m, 1H, C*H$_2$*), 1.55 (s, 2H, *H$_2$O*), 1.70 (m, 1H, C*H$_2$*), 1.90 (m, 2H, C*H$_2$*), 2.26 (s, 6H, NC*H$_3$*), 2.33 (br s, 6H, NC*H$_3$*), 2.47 (m, 2H, C*H$_2$*), 2.72 (s, 7H, NC*H$_3$* + 1 C*H*), 3.06 (s, 3H, NC*H$_3$*, $^3J_{HPt}$ = 22), 3.46 (s, 3H, NC*H$_3$*, $^3J_{HPt}$ = 17), 3.72 (m, 1H, C*H*), 6.74 (m, 2H, Ar), 7.09 (m, 1H, Ar), 7.3−7.9 (m, 11H, Ar), 8.35 (m, 1H, Ar), 9.37 (m, 1H, Ar). ^{31}P{^{1}H} NMR: δ 18.9 (d, $^1J_{PPt}$ = 3490, $^2J_{PP}$ = 12.3), 28.6 (d, $^1J_{PPt}$ = 3400, $^2J_{PP}$ = 12.3). Λ$_M$ (H$_2$O): 150. X-ray diffraction quality crystals of **2**·CH$_2$Cl$_2$·1.46H$_2$O were grown over 4 d by evaporation of a CH$_2$Cl$_2$ solution of the complex onto which EtOH had been layered (CH$_2$Cl$_2$:EtOH 2:5 by vol).

[PtCl(*P,P′,N*-dmapcp)]PF$_6$, 3. To a Schlenk tube charged with **2** (38 mg, 0.043 mmol) and NH$_4$PF$_6$ (7.0 mg, 0.043 mmol) was added acetone (10 mL). The resulting white suspension was stirred at room temperature (~20 °C) for 1 h and then filtered through Celite 545 that was washed with acetone (3 × 10 mL); the combined filtrate was reduced in vacuo to ~1 mL. The product was afforded as a white powder by the addition of Et$_2$O (20 mL), isolated by filtration, washed with Et$_2$O (3 × 3 mL), and dried in vacuo at 100 °C. Yield: 21 mg (49%). Anal. Calcd for C$_{37}$H$_{48}$N$_4$-ClF$_6$P$_3$Pt: C 45.1; H 4.9; N 5.7. Found: C 44.8; H 4.9; N 5.6. The solution ^{1}H NMR spectrum was essentially identical to that of **2**. ^{31}P{^{1}H} NMR: δ 17.0 (d, $^1J_{PPt}$ = 3510, $^2J_{PP}$ = 13.7), 26.7 (d, $^1J_{PPt}$ = 3390, $^2J_{PP}$ = 13.7), −145 (spt, $^1J_{PF}$ = 710, PF$_6^-$).

[PdCl(*P,P′,N*-dmapcp)]Cl, 4. To a Schlenk tube containing *trans*-PdCl$_2$(PhCN)$_2$ (55 mg, 0.14 mmol) and dmapcp (86 mg, 0.14 mmol) was added CH$_2$Cl$_2$ (10 mL), and the initially orange solution was stirred for 15 min when it became yellow. The volume was reduced to ~1 mL, and addition of Et$_2$O (20 mL) gave the yellow solid product that was isolated by filtration, washed with Et$_2$O (3 × 3 mL), and dried in vacuo. Yield: 109 mg (98%). Anal. Calcd for C$_{37}$H$_{48}$N$_4$Cl$_2$P$_2$Pd: C 56.4; H 6.1; N 7.1. Found: C 56.1; H 6.3; N 7.0. ^{1}H NMR: δ 1.42 (m, 1H, C*H$_2$*), 1.65 (br m, 1H, C*H$_2$*), 1.83 (br m, 1H, C*H$_2$*), 2.15 (br m, 1H, C*H$_2$*), 2.29 (s, 13H, NC*H$_3$*, and 1H, C*H$_2$*), 2.45 (br m, 1H, C*H$_2$*), 2.73 (s, 6H, NC*H$_3$*), 2.93 (s, 3H, NC*H$_3$*), 3.14 (br m, 1H, C*H*), 3.30 (s, 3H, NC*H$_3$*), 4.05 (br m, 1H, C*H*), 6.73 (m, 1H, Ar), 6.82 (pt, 1H, Ar), 7.08 (pt, 1H, Ar), 7.58 (m, 11H, Ar), 8.21 (pt, 1H, Ar), 9.43 (m, 1H, Ar). ^{31}P{^{1}H}

NMR: δ 48.7 (s), 49.6 (s) [$^2J_{PP}$ not resolved]. UV−vis: 334 [6100] (CH$_2$Cl$_2$); 378 [3900] (H$_2$O). Λ_M (H$_2$O): 200. A crystal of **4** was grown from a CH$_2$Cl$_2$ solution of the complex.

[PdI(P,P',N-dmapcp)]I, 5. To a Schlenk tube containing *trans*-PdCl$_2$(PhCN)$_2$ (71 mg, 0.19 mmol) and dmapcp (110 mg, 0.18 mmol) was added CH$_2$Cl$_2$ (5 mL), and the resulting orange solution was stirred for 0.5 h when it became yellow. To this was added NaI (97 mg, 0.65 mmol) and acetone (5 mL). The solution immediately became orange and turbid, and was stirred for a further 0.5 h, when the solvent was removed in vacuo. The residue was taken up in CH$_2$Cl$_2$ (10 mL), and the mixture was filtered through Celite 545. The filtrate volume was reduced to ∼2 mL, and addition of Et$_2$O (20 mL) precipitated the orange product that was collected by filtration, washed with Et$_2$O (3 × 3 mL), and dried in vacuo. Yield: 130 mg (74%). Anal. Calcd for C$_{37}$H$_{48}$N$_4$I$_2$P$_2$Pd: C, 45.8; H, 5.0; N, 5.8. Found: C, 45.9; H, 5.1; N, 5.6. ^{1}H NMR: δ 1.80 (br m, 2H, C*H*$_2$), 2.35 (br s, ∼12H, NC*H*$_3$), 2.70 (br s, ∼6H, NC*H*$_3$), 3.05 (br s, ∼3H, NC*H*$_3$), 3.70 (br s, ∼3H, NC*H*$_3$), 3.95 (br m, 1H, C*H*), 6.80 (br m, 1H, Ar), 7.05 (br m, 2H, Ar), 7.30−8.00 (br m, 11H, Ar), 8.20 (br m, 1H, Ar), 9.40 (br m, 1H, Ar). The peaks due to the remaining C*H*$_2$ and C*H* protons are obscured by the broad NC*H*$_3$ peaks. ^{31}P{^{1}H} NMR: δ 39.9 (s), 50.4 (s) [$^2J_{PP}$ not resolved].

[PdCl(P,P',N-dmapcp)]PF$_6$, 6. This complex was made in a manner corresponding to that given for **3,** except that a 5-fold excess of NH$_4$PF$_6$ was used. The acetone was removed at the pump and the residue taken up in CH$_2$Cl$_2$ (10 mL) before filtration through Celite 545. This removed unreacted NH$_4$PF$_6$ that is insoluble in CH$_2$Cl$_2$. Thus, reaction of **4** (150 mg, 0.19 mmol) and NH$_4$PF$_6$ (157 mg, 0.97 mmol) gave 171 mg (100%) of a yellow powder. Anal. Calcd for C$_{37}$H$_{48}$N$_4$ClF$_6$P$_3$Pd: C 49.5; H 5.4; N 6.2. Found: C 49.7; H 5.4; N 5.8. The ^{1}H NMR spectrum of **6** was essentially the same as that for **4**, and the ^{31}P{^{1}H} NMR spectrum was similarly identical save for the presence of the spt (δ −145) due to PF$_6^-$.

PtCl$_2$(dmape), 7. This complex was synthesized by the corresponding two routes detailed for **2.** Thus, reaction of PtCl$_2$ (105 mg, 0.40 mmol) and dmape (230 mg, 0.40 mmol) yielded 130 mg (40%) of a white powder, while reaction of PtCl$_2$(cod) (110 mg, 0.29 mmol) with dmape (160 mg, 0.28 mmol) gave 200 mg (85%) of **7**. However, elevated temperatures were not required for the latter preparation that was conducted in CH$_2$Cl$_2$ at room temperature. Anal. Calcd for C$_{34}$H$_{44}$N$_4$Cl$_2$P$_2$Pt: C 48.8; H 5.3; N 6.7; Found: C 48.5; H 5.3; N 6.5. **PtCl$_2$(P,P'-dmape), 7a:** ^{31}P{^{1}H} NMR (240 K): δ 46.0 (br s, $^1J_{PPt}$ = 3750). The ^{1}H NMR spectrum of **7a** was broad and uninformative, even at low temperature, and could not be resolved from that of [PtCl(P,P',N-dmape)]Cl (**7b**). Resonances of the NC*H*$_3$ and the CH$_2$ protons fell in the range δ 2−4, and the aromatic protons gave peaks between δ 6.5−9. **[PtCl-(P,P',N-dmape)]Cl, 7b:** ^{31}P{^{1}H} NMR (240 K): δ 32.0 (br s, $^1J_{PPt}$ = 3510), 53.0 (br s, $^1J_{PPt}$ = 3460). Evaporation over 3 d of a CH$_2$Cl$_2$ solution of **7** onto which EtOH had been layered (CH$_2$Cl$_2$:EtOH 1:1 by vol) yielded colorless, X-ray diffraction quality crystals of **7a·**CH$_2$Cl$_2$.

[PtCl(P,P',N-dmape)]PF$_6$, 8. This compound was prepared in the manner outlined for **6**. Thus, reaction of **7** (92 mg, 0.11 mmol) and NH$_4$PF$_6$ (42 mg, 0.26 mmol) gave 48 mg (47%) of a white powder. Anal. Calcd for C$_{34}$H$_{44}$N$_4$ClF$_6$P$_3$Pt: C 43.2; H 4.7; N 5.9. Found: C 43.3; H 4.9; N 5.8.^{1}H NMR: δ 2.2−3.6 (br m, 28H, C*H*$_2$ and NC*H*$_3$), 7.10−7.80 (br m, 12H, Ar), 8.05 (m, 4H, Ar). ^{31}P{^{1}H} NMR: δ 31.6 (s, $^1J_{PPt}$ = 3540), 52.7 (s, $^1J_{PPt}$ = 3446) [$^2J_{PP}$ not resolved], −145 (spt, $^1J_{PF}$ = 710, PF$_6^-$).

PdCl$_2$(dmape), 9. This complex was prepared in the same manner given for **4**. Thus, reaction of *trans*-PdCl$_2$(PhCN)$_2$ (56 mg, 0.15 mmol) and dmape (83 mg, 0.15 mmol) gave 88 mg (81%) of

a yellow powder. Anal. Calcd for C$_{34}$H$_{44}$N$_4$Cl$_2$P$_2$Pd: C 54.6; H 5.9; N 7.5; Found: C 54.6; H 5.9; N 7.6. The ^{1}H NMR spectra (CD$_2$Cl$_2$, 220−300 K) of an equilibrium mixture of the two isomers **9a** and **9b** were uninformative because the peaks were broad and overlapped. **PdCl$_2$(P,P'-dmape), 9a**: ^{31}P{^{1}H} NMR (CD$_2$Cl$_2$, 233 K): δ 66.4 (br s). **[PdCl(P,P',N-dmape)]Cl, 9b**: ^{31}P{^{1}H} NMR (CD$_2$Cl$_2$, 233 K): δ 60.5 (br s), 73.4 (br s). An X-ray quality crystal of **9a ·**CH$_2$Cl$_2$ was grown from a CH$_2$Cl$_2$ solution of the complex layered with Et$_2$O.

[PdCl(P,P',N-dmape)]PF$_6$, 10. This complex was prepared in the same manner outlined for **6**. Thus, reaction of **9** (83 mg, 0.11 mmol) and NH$_4$PF$_6$ (93 mg, 0.57 mmol) gave 60 mg (63%) of a yellow powder. Anal. Calcd for C$_{34}$H$_{44}$N$_4$ClF$_6$P$_3$Pd: C 47.6; H 5.2; N 6.5. Found: C 47.4; H 5.4; N 6.4. ^{1}H NMR: δ 2.6 (br s, ∼28H, CH$_2$ and NCH$_3$), 6.8−8.0 (br m, 16H, Ar). ^{31}P{^{1}H} NMR (CD$_2$-Cl$_2$): δ 60.5 (s), 73.4 (s) [$^2J_{PP}$ not resolved], and spt of PF$_6^-$.

[PdCl(P,P',N-dmape)]OTf, 11. To a CH$_2$Cl$_2$ solution (4 mL) of **9** (50 mg, 0.067 mmol) was added MeOTf (23 μL, 0.20 mmol), and the mixture was stirred at room temperature for 20 min. Volatiles were removed in vacuo, and the residue was dissolved in 0.5 mL of CH$_2$Cl$_2$. Precipitation with hexanes (∼20 mL) yielded a yellow, microcrystalline solid that was isolated, washed with Et$_2$O, and dried in vacuo. Yield: 31 mg (54%). Anal. Calcd for C$_{35}$H$_{44}$N$_4$-ClF$_3$O$_3$P$_2$PdS: C, 48.8; H, 5.1; N, 6.5. Found: C, 48.9; H, 5.2; N, 6.4. ^{1}H NMR (CD$_2$Cl$_2$): δ 1.68 (s, 4H, C*H*$_2$), 2.63 (s, 18H, NC*H*$_3$), 3.49 (s, 6H, NC*H*$_3$), 7.34−7.82 (m, 16H, Ar). ^{31}P{^{1}H} NMR (CD$_2$-Cl$_2$): δ 61.0 (s), 73.8 (s) [$^2J_{PP}$ not resolved]. ^{19}F NMR (CD$_2$Cl$_2$): δ −78.6 (s). IR: ν_{SO} 1260. The triflate derivative was made because an X-ray quality crystal of **11·**CH$_2$Cl$_2$ could be grown from a CH$_2$-Cl$_2$ solution of the complex layered with Et$_2$O.

[Pd(μ-Cl)(P,P'-dmapm)]$_2$[PF$_6$]$_2$, 12. To a CH$_2$Cl$_2$ (4 mL) solution containing PdCl$_2$(dmapm) (**1**) (110 mg, 0.15 mmol) was added acetone (6 mL) and NH$_4$PF$_6$ (220 mg, 1.3 mmol). The resulting orange slurry was stirred at room temperature for 3 h and then reduced in vacuo to a residue that was taken up in CH$_2$Cl$_2$ (∼5 mL), prior to filtration through Celite 545. The orange filtrate was reduced to ∼1 mL, and EtOH (10 mL) was added to precipitate the orange product. Addition of Et$_2$O (10 mL) gave further product that was isolated by filtration, washed with Et$_2$O (3 × 3 mL), and dried in vacuo. Yield: 77 mg (61%). Anal. Calcd for C$_{66}$H$_{84}$N$_8$-Cl$_2$F$_{12}$P$_6$Pd$_2$: C, 47.0; H, 5.0; N, 6.6. Found: C, 47.1; H, 5.0; N, 6.6. UV−vis (CH$_2$Cl$_2$): 360 [14600]. ^{1}H NMR: δ 2.56 (s, 48H, NC*H*$_3$), 4.91 (t, 4H, C*H*$_2$, $^2J_{HP}$ = 12.3), 7.32 (m, 16H, Ar), 7.57 (pt, 8H, Ar), 7.97 (m, 8H, Ar). ^{31}P{^{1}H} NMR: δ −52.0 (s), and spt of PF$_6^-$. Λ_M (MeNO$_2$): 213.

X-ray Crystallographic Analyses. Measurements were made on a Rigaku/ADSC CCD diffractometer at 180(1) K (for **2·**CH$_2$-Cl$_2$·1.46H$_2$O, **4** and **7a·**CH$_2$Cl$_2$), or 173(1) K (for **9a·**CH$_2$Cl$_2$and **11·**CH$_2$Cl$_2$) using graphite monochromated Mo Kα radiation (λ = 0.71069 Å). Some crystallographic data are shown in Table 1. The data were collected and processed using the d*TREK program,[26a] and the structures were solved using heavy- atom Patterson[26b] (for

(26) (a) *d*TREK: Area Detector Software*; Molecular Structure Corporation: The Woodlands, TX, 1997. (b) Beurskens, P. T.; Admiraal, G.; Beurskens, G.; Bosman, W. P.; Garcia-Granfa, S.; Gould, R. O.; Smits, J. M. M.; Smykalla, C. *The DIRDIF−PATTY−Program System*; Technical Report of the Crystallography Laboratory; University of Nijmegen: Nijmegen, The Netherlands, 1992. (c) Altomare, A.; Burla. M. C.; Cammalli, G.; Cascarano, M.; Giacovazzo, C.; Guagliardi, A.; Moliterni, A. G. G.; Polidori, G.; Spagna, A. *J. Appl. Crystallogr.* **1999**, *32*, 115. (d) Beurskens, P. T.; Admiraal, G.; Beurskens, G.; Bosman, W. P.; de Gelder, R.; Israel, R.; Smits, J. M. M. *The DIRDIF-94 Program System*; Technical Report of the Crystallography Laboratory; University of Nijmegen: Nijmegen, The Netherlands, 1994.

Table 1. Crystallographic Data for **2**·CH$_2$Cl$_2$·1.46H$_2$O, **7a**·CH$_2$Cl$_2$, **9a**·CH$_2$Cl$_2$, and **11**·CH$_2$Cl$_2$

	2·CH$_2$Cl$_2$·1.46H$_2$O	**7a**·CH$_2$Cl$_2$	**9a**·CH$_2$Cl$_2$	**11a**·CH$_2$Cl$_2$
formula	C$_{38}$H$_{52.92}$Cl$_4$N$_4$P$_2$PtO$_{1.46}$	C$_{35}$H$_{46}$Cl$_4$N$_4$P$_2$Pt	C$_{35}$H$_{46}$Cl$_4$N$_4$P$_2$Pd	C$_{36}$H$_{46}$Cl$_3$N$_4$O$_3$F$_3$P$_2$SPd
fw	987.99	921.62	832.93	946.55
cryst color, habit	colorless, irregular	colorless, prism	yellow, block	colorless, plate
cryst size (mm^3)	0.15 × 0.20 × 0.25	0.15 × 0.20 × 0.25	0.50 × 0.40 × 0.20	0.30 × 0.25 × 0.10
space group	$P\bar{1}$ (#2)	$P2_1$ (#4)	$P2_1$ (#4)	$P\bar{1}$ (#2)
a (Å)	10.6530(8)	12.3471(14)	12.3010(3)	9.9087(9)
b (Å)	14.115(2)	11.8502(13)	11.8069(3)	11.2071(4)
c (Å)	14.998(2)	12.9845(2)	12.9733(4)	20.076(1)
α (deg)	71.471(4)	−	−	87.556(2)
β (deg)	78.1136(14)	94.7052(4)	94.607(2)	86.209(2)
γ (deg)	79.2564(13)	−	−	70.624(2)
V (Å^3)	2074.5(4)	1893.4(2)	1878.1(2)	2098.1(2)
Z	2	2	2	2
μ (cm^{-1})	37.39	40.88	8.95	8.12
total reflns	19383	14846	16349	18870
unique reflns	9355	7628	7915	8457
R_{int}	0.046	0.021	0.035	0.040
no. variables	499	414	414	456
R1 ($I > n\sigma(I)$)^a	0.032 ($n = 3$, 6381 obsd reflns)	0.041($n = 0$, 7603 obsd reflns)	0.022 ($n = 3$, 7647 obsd reflns)	0.038 ($n = 2$, 6943 obsd reflns
wR2^b	0.054	0.046	0.062	0.096
GOF	1.05	1.24	1.09	1.06

^{a} R1 = $\Sigma||F_o| - |F_c||/\Sigma|F_o|$ (observed data). ^{b} wR2 = $[\Sigma(F_o^2 - F_c^2)^2/\Sigma w(F_o^2)^2]^{1/2}$ (all data).

2 and **7a**) or direct[26c] (for **9a** and **11**) methods, and expanded using Fourier techniques.[26d]

Protocol for the Catalytic Hydration of Maleic Acid, *cis*-CH-(CO$_2$H)=CH(CO$_2$H). To a combination of maleic acid (116 mg, 1.00 mmol) and a selected metal complex (0.01 mmol) in a 5 mm-wall Schlenk tube (∼30 cm in length), topped with a Teflon Kontes valve, and having a sidearm gas inlet and magnetic stir bar, was added H$_2$O (10 mL). The solution was degassed by shaking the vessel under vacuum, and then Ar (1 atm) was admitted. The tube was kept at 100 °C, and after 24 h, a 3 mL aliquot was withdrawn. This was reduced to dryness on a rotatory evaporator and the residue was ground to a powder sample (∼7 mg) that was dissolved in acetone-d_6 (0.5 mL) to acquire a ^{1}H NMR spectrum. The proportions of maleic, fumaric (the *trans*-isomer), and malic (the hydration product, hydroxysuccinic) acids present were calculated using the ratios of appropriate peak integrations (δ, acetone-d_6: maleic, 6.40 s, *cis*-C*H*=C*H*; fumaric, 6.80 s, *trans*-C*H*=C*H*; malic, 4.52 dd, C*H*(OH)CH$_2$).

Results and Discussion

Complexes of dmapcp. Reaction of dmapcp with PtCl$_2$ or PtCl$_2$(cod) gives the white, air-stable, water-soluble complex, [PtCl(*P,P′,N*-dmapcp)]Cl (**2**). The complex analyzed as a monohydrate, and ^{1}H NMR confirmed the presence of H$_2$O; moreover, crystals of **2** contained 1.46H$_2$O per unit cell (see below). The number and relative integrations of the singlets due to the NC*H*$_3$ protons in the ^{1}H NMR spectra of anilinyldiphosphine complexes constitute an invaluable diagnostic tool for determining the overall solution structure of the molecule. In free dmapcp, the two anilinyl substituents on each P-atom are diastereotopic, related to those on the opposite P-atom by a C_2 axis: the ligand bears homotopic pairs of diastereotopic anilinyl rings, and the ^{1}H NMR spectrum shows two singlets for the NC*H*$_3$ protons (δ 2.55 and 2.63).[8] In the case of **2**, the C_2 symmetry is lifted, and four sharp peaks due to NC*H*$_3$ protons are apparent at δ 3.46, 3.06, 2.72, and 2.26 in a 1:1:2:2 ratio (i.e., 3:3:6:6 protons). The remaining six NC*H*$_3$ protons are manifested by a broad peak at δ 2.33 (Figure 1). This pattern of NC*H*$_3$

peaks defines a *P,P′,N*- coordination mode that is shown in Chart 2 together with ^{1}H NMR peak assignments. On the

Chart 2. Labeling of the NMe Groups in the Cation of **2**
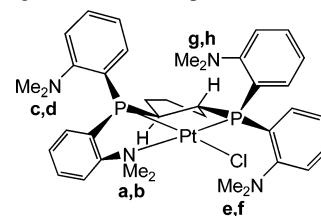
basis of integration, the two most downfield singlets (equivalent to three protons each) are assigned unequivocally to Me groups **a** and **b** associated with the Pt-bound N-atom: these peaks show the largest coordination shifts from their (average) position in the free ligand ($\Delta\delta = 0.83$ and 0.51 ppm), and they show three-bond ^{1}H−^{195}Pt coupling (17 and 22 Hz, respectively).
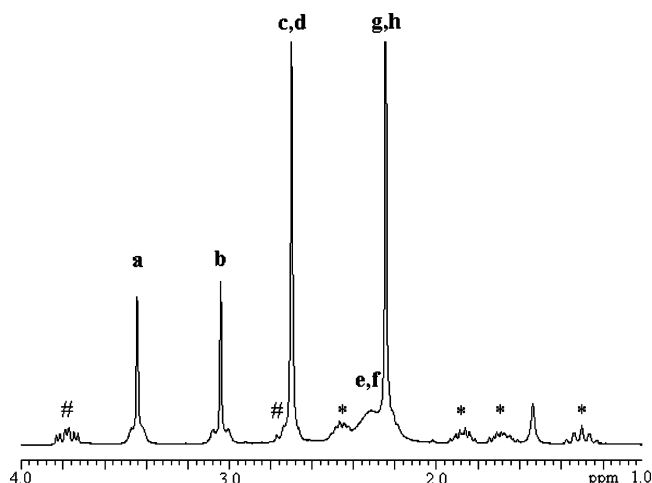
Figure 1. The δ 1−4 region of the ^{1}H{^{31}P} NMR spectrum (121 MHz, CDCl$_3$, 300 K) of [PtCl(*P,P′,N*-dmapcp)]Cl (**2**); (*) and (#) indicate peaks due to the C*H*$_2$ and C*H* protons. Assignments (**a**−**h**) are discussed in the text and shown in Chart 1. The singlet at δ 1.55 is due to H$_2$O.
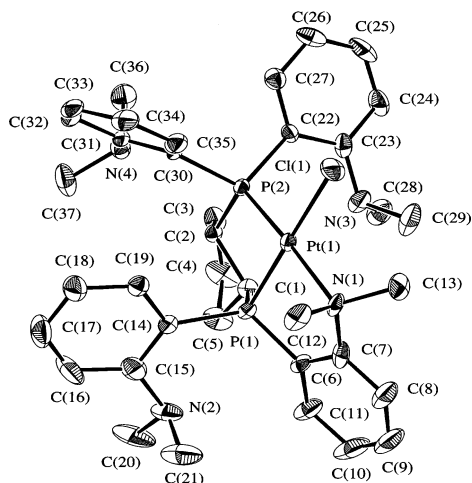
Figure 2. ORTEP representation (50% ellipsoids) of the cation of [PtCl-(*P,P′,N*-dmapcp)]Cl (**2**) showing the *P,P′,N*-coordination; H-atoms are omitted for clarity.

Table 2. Selected Bond Distances and Angles for **2·**CH$_2$Cl$_2$·1.46H$_2$O with Estimated Standard Deviations in Parentheses

Pt(1)−P(1)	2.2012(12)	Pt(1)−P(2)	2.2646(10)
Pt(1)−N(1)	2.184(3)	Pt(1)−Cl(1)	2.3642(13)
P(1)−C(1)	1.822(4)	P(1)−C(6)	1.782(4)
P(1)−C(14)	1.814(5)	P(2)−C(2)	1.848(4)
P(2)−C(22)	1.819(5)	P(2)−C(30)	1.829(4)
N(1)−C(7)	1.481(6)	N(1)−C(12)	1.490(6)
N(1)−C(13)	1.496(6)	N(2)−C(15)	1.452(6)
N(2)−C(20)	1.500(6)	N(2)−C(21)	1.449(6)
P(1)−Pt(1)−N(1)	84.07(11)	P(2)−Pt(1)−Cl(1)	94.08(4)
P(1)−Pt(1)−P(2)	87.43(4)	Cl(1)−Pt(1)−N(1)	94.53(11)
C(1)−P(1)−C(6)	112.1(2)	C(1)−P(1)−C(14)	109.1(2)
C(6)−P(1)−C(14)	115.9(2)	C(12)−N(1)−C(13)	109.8(3)
C(7)−N(1)−C(12)	108.3(4)	C(7)−N(1)−C(13)	109.2(4)
C(20)−N(2)−C(15)	114.6(4)	C(20)−N(2)−C(21)	109.5(4)
C(15)−N(2)−C(21)	109.9(4)	C(1)−C(5)−C(4)	99.3(4)
C(5)−C(4)−C(3)	106.2(4)	C(4)−C(3)−C(2)	105.8(4)
P(1)−C(1)−C(5)	125.4(3)	P(2)−C(2)−C(3)	123.8(3)

The structure of the cation component of **2·**CH$_2$Cl$_2$·1.46H$_2$O is shown in Figure 2, and selected bond distances and angles are given in Table 2. The metal coordination sphere is approximately square planar and, in agreement with the solution NMR data, the ligand adopts a *P,P′,N*-configuration in the solid state. The absolute configurations of P(1) and the methine C-atoms C(1) and C(2) are *R,S,S*, respectively, and the five-membered chelate ring is in the δ-configuration. As the space group is *P*1(bar) and *Z* = 2, the mirror image is present in the unit cell, but the diastereomeric *R,R,R* and *S,S,S* forms are absent. This is consistent with the fact that the substituents on the P-atoms of a chiral *C*$_2$-symmetric ligand are present as pseudoaxial and pseudoequatorial pairs, and the hypothesis that only the equatorial type are sterically available for binding to a square planar metal center. That the *R,R,R* and *S,S,S* forms of **2** cannot arise was shown by a 2D ^{1}H EXSY experiment [see Figure S1 in the Supporting Information (SI)]. If the "pendant" and bound N-atoms were in free chemical exchange, the stereogenic P-atoms would be racemized. If, however, only pseudoequatorial anilinyl rings are able to bind to the Pt, then the *N*Me groups **a** and **b** cannot exchange with **c** and **d**, i.e., the *N*Me groups associated with the other (pseudoaxial) anilinyl group attached to the same (bound) P-atom. Rather, **a** and **b** can only

Scheme 1. Exchange of Free and Coordinated Anilinyl Groups in the Cation of [PtCl(*P,P′,N*-dmapcp)]Cl (**2**)^a
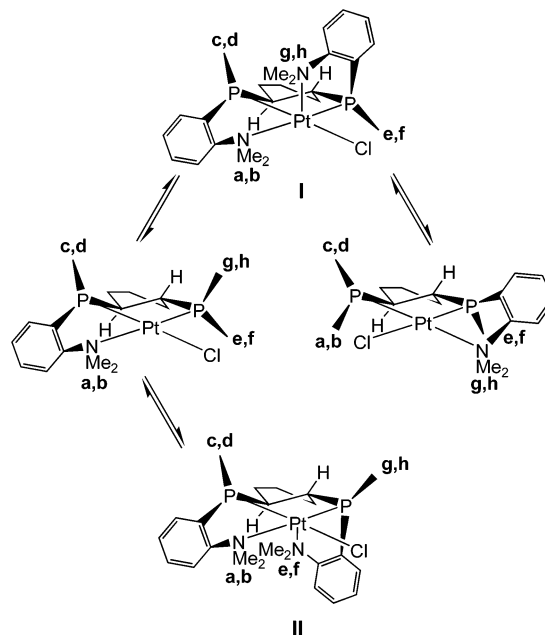
^{a} For clarity only bonding anilinyl rings are shown; the pendant rings are omitted, as well as the cation +1 charge.

be in exchange with the *N*Me protons of the corresponding pseudoequatorial anilinyl ring on the other P-atom. This is clearly demonstrated by the EXSY NMR spectrum: **a** and **b** are in chemical exchange with **g,h** only, while **c,d** and **e,f** are mutually exchanging. If an associative mechanism is assumed for the d^8 square planar metal center, the data can be interpreted via the exchange pathways illustrated in Scheme 1. Only one diastereomer (**I**) of the postulated five-coordinate *P,P′,N,N′*-intermediate, arising from coordination of N(4) (Figure 2), can lead to the exchange of P-atoms. Inspection of the crystal structure shows no obvious reason why the "nonproductive" diastereomer (**II**) should not also form; however, this cannot decay to **2**, probably for reasons of steric strain at the P(2)-atom. The broadened ^{1}H NMR peak due to the **e,f** groups is tentatively attributed to the rapid equilibrium formation of **II**, i.e., to the reversible binding of N(3) (Figure 2).

Complexes bearing *P,P,N*-chelating ligands, in which the *N*-donor is pendant from one of the *P*-donors, are known,[6] including *P,N,P*-pincer[27] and *P,P,N*-tripod[28] type systems. An example relevant to this paper is the five-coordinate Rh-(I) compound *meso*-[Rh(cod)(*P,P′,N*-Ph$_2$P{CH(py)}$_2$PPh$_2$)]$^+$ (py = *o*-pyridyl), in which there is slow interchange of coordinated and noncoordinated pyridyl rings,[29] very much like the exchange seen in **2**. A key difference between the Rh system and **2** is that, in the former, exchange of the bound and free N-atoms results in the conversion of one enantiomer into the other, while in **2**, it results in self-exchange. The inability of the P-atom to epimerize during the fluxional

(27) Melaimi, M.; Thoumazet, C.; Ricard, L.; LeFloch, P. *J. Organomet. Chem.* **2004**, *689*, 2988 and refs. therein.
(28) Liu, C.-Y.; Cheng, M.-C.; Peng, S.-M.; Liu, S.-T. *Organometallics* **1994**, *13*, 4294.
(29) Bookham, J. L.; Smithies, D. M.; Thornton Pett, M. *J. Chem. Soc., Dalton Trans.* **2000**, 975.

process is obviously of importance for potential asymmetric catalysis using ligands such as dmapcp. A detailed understanding of the stereochemical implications of fluxional processes in chiral complexes is becoming increasingly important in light of recent discoveries that both chiral[30] and achiral[31] hemilabile ligand groups may act to enhance enantioselectivities in metal-catalyzed asymmetric reactions.

The aqueous conductivity of **2** is 150 ohm^{-1} mol^{-1} cm^2, consistent with a 1:1 electrolyte,[32] and the Cl$^-$ anion is easily replaced by PF$_6^-$ on reaction with NH$_4$PF$_6$ in acetone at room temperature to give [PtCl(P,P',N-dmapcp)]PF$_6$ (**3**). Even in the presence of excess NH$_4$PF$_6$, only the ionic chloride of **2** is replaced under these conditions.

The dmapcp ligand reacts in an analogous fashion with *trans*-PdCl$_2$(PhCN)$_2$ to give the yellow, air-stable, water-soluble complex, [PdCl(P,P',N-dmapcp)]Cl (**4**). Olefin-free Pd precursors are preferable to PdX$_2$(diolefin) (X = halogen) for the syntheses of the Pd complexes because the *o*-anilinyldiphosphine ligands tend to react with coordinated olefin, most probably via nucleophilic attack by either the P-atom[33,34] or N-atom.[35] Thus, dmapcp reacts with PdCl$_2$(cod) at room temperature to give not only **4**, but also another product (**A**) with an AX pattern in the ^{31}P{^{1}H} NMR spectrum: δ_A 36.5 (d), δ_X 47.8 (d), $^2J_{PP}$ = 8.8 Hz. As the ^{31}P{^{1}H} NMR spectrum of **A** depends both on the nature of the diolefin, and the ^{1}H NMR shows peaks of coordinated olefin (multiplets at δ 5.23, 5.65),[36] **A** must be an organometallic species bearing both the diolefin moiety and the anilinyldiphosphine ligand; a plausible suggestion for the structure of **A** is given in the Supporting Information (Chart S1). Further studies are needed to substantiate this organometallic chemistry.

The ^{1}H NMR spectrum of **4** is reminiscent of that of **2**, but shows only four NCH_3 peaks in a 1:1:2:4 ratio. The difference arises from overlap of peaks due to the **e,f** and **g,h** groups of NCH$_3$ protons in **4**. A P,P',N coordination mode of dmapcp is indicated, and this was confirmed by some crystallographic data; these are not good enough for publication, but at least the atom connectivity is established (Figure S2 shows a PLUTO representation of the structure, while a well determined structure of the [PdCl(P,P',N-dmape)]$^+$ cation in **11** is discussed below). However, the ^{31}P{^{1}H} spectrum shows two closely separated singlets at δ 48.7 and 49.6 instead of the anticipated AX pattern (as seen for the Pt analogue, **2**; see Figure S3). The 2D ^{1}H EXSY spectrum of **4** is similar to that of **2**, implying similar exchange between coordinated and free anilinyl N-atoms. The ^{31}P{^{1}H} data suggest that the P-atoms are undergoing exchange. Such exchange between P-atoms whose pendant N-containing "arms" are either coordinated or free has been

(30) Zhang, A.; Rajanbabu, T. V. *Org. Lett.* **2004**, *6*, 1515.
(31) Goldfuss, B.; Löschmann, T.; Rominger, F. *Chem. Eur. J.* **2004**, *10*, 5422.
(32) Geary, W. J. *Coord. Chem. Rev.* **1971**, *7*, 81.
(33) Fallis, S.; Anderson, G. K.; Rath, N. P. *Organometallics* **1991**, *10*, 3180.
(34) Huang, C.-C.; Duan, J.-P.; Wu, M.-Y.; Liao, F.-L.; Wang, S.-L.; Cheng, C.-H. *Organometallics* **1998**, *17*, 676.
(35) Panunzi, A.; Renzi, A. D.; Paiaro, G. *J. Am. Chem. Soc.* **1970**, *92*, 3488.
(36) Jones, N. D.; James, B. R. *Can. J. Chem.* In press.

Scheme 2. MCl$_2$(P,P'-dmape) ⇌ [MCl(P,P',N-dmape)][Cl] Equilibria for **7a,b** (M = Pt) and **9a,b** (M = Pd)
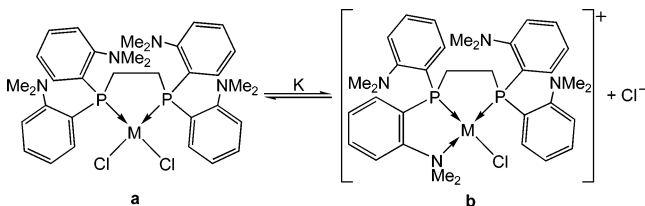
observed by Stelzer and co-workers[37] for the compound [PdCl(P,P',N-py(CH$_2$)$_2$P(Me)(CH$_2$)$_3$P(Me)(CH$_2$)$_2$py)]Cl (py = *o*-pyridyl), which gives two ^{31}P{^{1}H} singlets at δ 13.7 and 15.5; and just as **2** gives the AX pattern, the analogous Pt complex of Stelzer gives two separated signals for the chemically inequivalent P-atoms at δ −6.2 and −12.9.

Reaction of **4** with excess NaI gives [PdI(P,P',N-dmapcp)]I (**5**) and with NH$_4$PF$_6$ gives [PdCl(P,P',N-dmapcp)]PF$_6$ (**6**). In water, the molar conductivity of **4** is 200 ohm^{-1} cm^2 mol^{-1}, perhaps indicating further chloride dissociation to generate [Pd(OH$_2$)(P,P',N-dmapcp)]Cl$_2$; the bathochromic shift in λ_{max} on going from CH$_2$Cl$_2$ (334 nm) to H$_2$O (378 nm) also suggests a change in inner-sphere coordination on dissolution of **4** in H$_2$O.

Complexes of dmape. The isolated product **7** from the 1:1 reaction between dmape and PtCl$_2$(cod) exists in CDCl$_3$ solution as a mixture of PtCl$_2$(P,P'-dmape) (**7a**) and [PtCl-(P,P',N-dmape)]Cl (**7b**). At room temperature, the ^{31}P{^{1}H} NMR spectrum consists of several broad, ill-defined peaks in the range δ 15−70; however, below ∼250 K, this resolves into three singlets and their associated Pt satellites (Figure S4). The peaks at δ 32 and 53 correspond to the inequivalent P-atoms of **7b**, as shown by room temperature ^{31}P{^{1}H} data (δ 31.6 and 52.7) for [PtCl(P,P',N-dmape)]PF$_6$ (**8**), made from **7** by treatment with NH$_4$PF$_6$. As for the dmapcp analogues **4** and **6**, $^2J_{PP}$ coupling was not observed for **7b** or **8**. The remaining singlet (δ 46) at 240 K corresponds to the C_2-symmetric complex **7a**. No evidence was obtained for formation of [Pt(P,P',N,N'-dmape)]Cl$_2$.

The Pd product (**9**) from reaction of dmape and *trans*-PdCl$_2$(PhCN)$_2$ exhibited NMR behavior analogous to that of **7**. The room temperature ^{31}P{^{1}H} spectrum showed a single broad peak centered at δ 66.4 that below ∼250 K diminished in intensity with 2 new singlets at δ 60.5 and 73.4 appearing, these corresponding to the resonances of the separately synthesized [PdCl(P,P',N-dmape)]PF$_6$ (**10**). Thus, the δ 66.4 singlet is assigned to PdCl$_2$(P,P'-dmape) (**9a**), and those at δ 60.5 and 73.4 to the inequivalent P-atoms of [PdCl-(P,P',N-dmape)]Cl (**9b**) (where again $^2J_{PP}$ is unresolved).

Variable temperature, reversible ^{31}P{^{1}H} NMR spectra of **7** and **9** in CD$_2$Cl$_2$ showed that the P,P'- (**a**) and P,P',N-isomers (**b**) are in thermal equilibrium (Scheme 2), and equilibrium constants (K) were determined for both systems from the spectra over the temperature range 210−250 K; the resulting van't Hoff plots appear in Figure S5. The determined thermodynamic parameters are $\Delta H°$ = −19 ±

(37) Hessler, A.; Fischer, J.; Kucken, S.; Stelzer, O. *Chem. Ber.* **1994**, *127*, 481.

4 kJ mol^{-1} and $\Delta S° = -100 \pm 30$ J mol^{-1} K^{-1} for **7**, and $\Delta H° = -11 \pm 7$ kJ mol^{-1} and $\Delta S° = -60 \pm 20$ J mol^{-1} K^{-1} for **9**. The entropy decrease likely results from solvent ordering about the charged species, and the exothermicity presumably reflects the formation of strong M−N bonds (vs M-Cl) with that for Pt being stronger than for Pd.

Because of the equilibria between the neutral dichloro and cationic monochloro species, the ^{1}H NMR resonances (particularly of the CH$_2$ protons) were broadened and difficult to assign.

More generally, studies on hemilabile ligands (that can make available a coordination site as needed) remain highly topical, because of their ability to confer on metal complexes the balance between stability and a reactivity needed for a catalytic system.[15] Hemilability has been assessed historically in terms of rates of intramolecular exchange between coordinated and pendant groups, studied usually by variable temperature NMR line-shape analysis;[38] such kinetic data often refer to exchange between identical or enantiomeric complexes ("Type II" hemilability as defined by Braunstein and Naud[15]). Equilibria thermodynamic data of the kind shown in Scheme 2, where there is competition for a metal center between a hemilabile group and an incoming (intermolecular) ligand, are rare,[39] although many processes of this type (Type III)[15] have been observed[40] and are especially relevant to catalysis in terms of designing hemilabile ligands. Of note, the hemilabile nature of the dmape systems (Scheme 2) is quite different from that of the dmapm ones, which is governed by the strain energy of the four-membered metal-chelate ring[10] (see below).

The X-ray crystallographic structure of **7a**·CH$_2$Cl$_2$ (Figure 3, Table 3) reveals the expected, close to square planar coordination at the metal. Bond distances and angles are similar to those of other Pt^{II} complexes with bis(phosphine) ligands.[41] All four anilinyl groups are involved in short intramolecular C−H···N contacts involving the ligand CH$_2$ protons, these interactions being reminiscent of those seen in the free ligands.[8] The Pd analogue, **9a**·CH$_2$Cl$_2$ (Figure 4, Table 4), is isostructural with **7a**·CH$_2$Cl$_2$, the bond lengths and angles being within 0.015 Å and 3.0°, respectively, of those of the Pt system. Distances of ∼3.65 Å between the metal atom and the N-atom of a noncoordinating dimethylanilinyl group in the structures of **7a** (Pt−N(1)) and **9a** (Pd−N(3)) are slightly less than the sum of the van der Waals radii of the metal and N-atom (3.85 Å)[42] and presumably this weak interaction assists in the loss of coordinated chloride to form **7b** and **9b**, respectively.
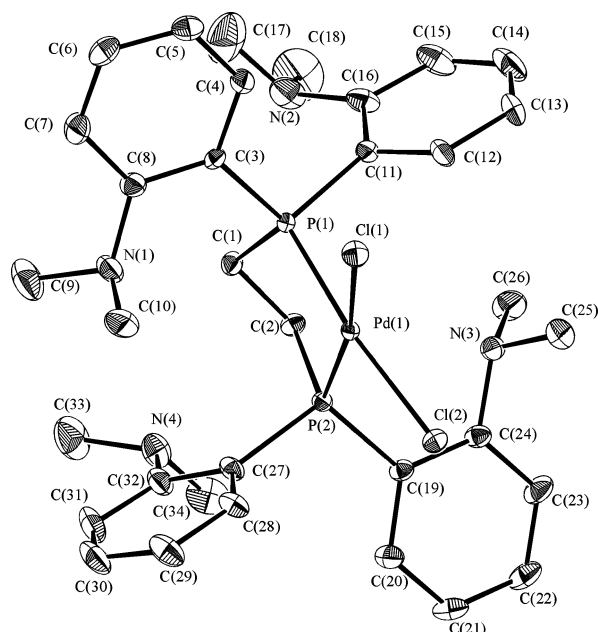
(38) For example: Lindner, E.; Möckel, A.; Mayer, H. A.; Kühbauch, H.; Fawzi, R.; Steimann, M. *Inorg. Chem.* **1993**, *32*, 1266.
(39) We have been unable to find a report showing such thermodynamic data; the closest system is our own work (ref 10) that involves the intramolecular ligand system PdCl$_2$(P, P-dmapm) ⇌ PdCl$_2$(P, N-dmapm).
(40) For *P, N*-systems, see for example: Braunstein, P.; Naud, F.; Dedieu, A.; Rohmer, M.-M.; DeCian, A.; Rettig, S. J. *Organometallics* **2001**, *20*, 2966. Braunstein, P.; Naud, F.; Rettig, S. J. *New J. Chem.* **2001**, *25*, 32. Cadierno, V.; Díez, J.; García-Garrido, S. E.; García-Granda, S.; Gimeno, J. *J. Chem. Soc., Dalton Trans.* **2002**, 1465.
(41) Orpen, A. G.; Brammer, L.; Allen, F. H.; Kennard, O.; Watson, D. G. J. *Chem. Soc., Dalton Trans.* **1989**, S1.
(42) Bondi, A. *J. Phys. Chem.* **1964**, *68*, 441.

Figure 3. ORTEP representation (50% ellipsoids) of PtCl$_2$(P,P′-dmape) (**7a**). The C−H···N contacts involving the CH$_2$ protons are shown; other H-atoms are omitted.

Table 3. Selected Bond Distances and Angles for **7a**·CH$_2$Cl$_2$ with Estimated Standard Deviations Parentheses

Pt(1)−P(1)	2.2317(13)	Pt(1)−P(2)	2.2355(13)
Pt(1)−Cl(1)	2.3728(12)	Pt(1)−Cl(2)	2.3776(13)
P(1)−C(1)	1.8819(5)	P(1)−C(3)	1.810(4)
P(1)−C(11)	1.818(7)	P(2)−C(2)	1.833(5)
P(2)−C(19)	1.844(7)	P(2)−C(27)	1.813(4)
P(1)−Pt(1)−Cl(2)	92.74(5)	P(2)−Pt(1)−Cl(1)	91.25(5)
P(1)−Pt(1)−P(2)	86.07(5)	Cl(1)−Pt(1)−Cl(2)	90.99(5)
C(1)−P(1)−C(3)	109.2(2)	C(3)−P(1)−C(11)	105.5(3)
C(11)−P(1)−C(1)	109.2(3)	C(2)−P(2)−C(19)	106.2(3)
C(19)−P(2)−C(27)	105.7(3)	C(2)−P(2)−C(27)	110.2(2)

A suitable crystal to substantiate the structure of the cation in **9b** was obtained from a CH$_2$Cl$_2$ solution of the triflate salt, [PdCl(P,P′,N-dmape)]OTf (**11**), this being readily

Figure 4. ORTEP representation (50% ellipsoids) of PdCl$_2$(P,P′-dmape) (**9a**); H-atoms are omitted for clarity.

Table 4. Selected Bond Distances and Angles for **9a**·CH₂Cl₂ with Estimated Standard Deviations Parentheses

Pd(1)−P(1)	2.2507(5)	Pd(1)−P(2)	2.2471(5)
Pd(1)−Cl(1)	2.3690(5)	Pd(1)−Cl(2)	2.3783(5)
P(1)−C(1)	1.836(2)	P(1)−C(3)	1.815(2)
P(1)−C(11)	1.833(2)	P(2)−C(2)	1.830(2)
P(2)−C(19)	1.813(2)	P(2)−C(27)	1.836(2)
P(1)−Pd(1)−Cl(1)	90.42(2)	P(2)−Pd(1)−Cl(2)	92.16(2)
P(1)−Pd(1)−P(2)	85.13(2)	Cl(1)−Pd(1)−Cl(2)	93.43(2)
C(1)−P(1)−C(11)	106.5(1)	C(3)−P(1)−C(11)	105.9(1)
C(11)−P(1)−C(3)	105.9(1)	C(2)−P(2)−C(19)	108.79(9)
C(19)−P(2)−C(27)	105.7(1)	C(2)−P(2)−C(27)	109.2(1)

Table 5. Selected Bond Distances and Angles for **11**·CH₂Cl₂ with Estimated Standard Deviations Parentheses

Pd(1)−P(1)	2.1833(8)	Pd(1)−P(2)	2.2457(8)
Pd(1)−N(1)	2.191(2)	Pd(1)−Cl(1)	2.3578(8)
P(1)−C(17)	1.825(3)	P(1)−C(9)	1.808(3)
P(1)−C(1)	1.797(3)	P(2)−C(18)	1.850(3)
P(2)−C(27)	1.804(3)	P(2)−C(19A)	1.839(3)
N(1)−C(2)	1.472(4)	N(1)−C(8)	1.501(4)
N(1)−C(7)	1.481(4)	N(2)−C(10)	1.437(4)
N(2)−C(16)	1.470(4)	N(2)−C(15)	1.466(4)
P(1)−Pd(1)−N(1)	85.90(7)	P(2)−Pd(1)−Cl(1)	96.59(3)
P(1)−Pd(1)−P(2)	83.17(3)	Cl(1)−Pd(1)−N(1)	94.83(7)
C(17)−P(1)−C(1)	112.80(13)	C(17)−P(1)−C(9)	106.68(13)
C(1)−P(1)−C(9)	110.48(13)	C(7)−N(1)−C(8)	108.9(3)
C(2)−N(1)−C(7)	110.9(2)	C(2)−N(1)−C(8)	108.9(2)
C(15)−N(2)−C(10)	112.9(3)	C(15)−N(2)−C(16)	108.9(3)
C(16)−N(2)−C(10)	110.3(3)		

formed by treatment of **9** (the isomeric mixture) with MeOTf. As in the case of Cl⁻ abstraction with NH₄PF₆, only one Cl⁻ is removed by excess (~3-fold) MeOTf. The structure of **11** (Figure 5, Table 5) is very similar to that of **2** and shows the *P,P′,N*-coordination with distortion from square planarity at the metal (one of the anilinyl rings at P(2) is disordered in two orientations). For the structure shown in Figure 5, the absolute configuration of P(1) is *R*, and the five-membered chelate ring is again in the δ-configuration, but the *P*1(bar) space group with *Z* = 2 implies again that the mirror image molecule (where the configuration of P(1) is *S*) is also present in the unit cell. Complex **11** is soluble in chlorinated solvents and acetone and is slightly soluble in water. The unresolved ³¹P{¹H} NMR spectrum for the
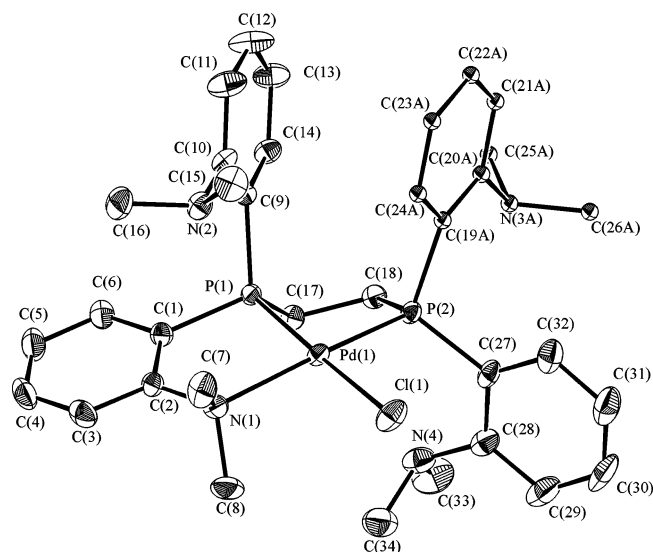
Figure 5. ORTEP representation (50% ellipsoids) of the cation of [PdCl-(*P,P′,N*-dmape)]OTf (**11**); H-atoms are omitted for clarity.

Chart 3. Hydration of Maleic to Malic Acid

Maleic Acid ⟶ Malic Acid
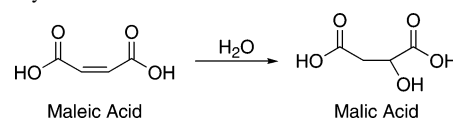
Table 6. Product Distributions for Catalytic Hydration of Maleic Acid[a]

catalyst precursor	maleic acid (%)	fumaric acid (%)	malic acid (%)
none	95	3	2
HCl (1.2 M)	78	16	6
[PtCl(*P,P′,N*-dmapcp)]Cl (**2**)	91	4	5
[PdCl(*P,P′,N*-dmapcp)]Cl (**4**)	88	6	6
[PdI(*P,P′,N*-dmapcp)]I (**5**)	93	4	3
PdCl₂(dmape) (**9**)	92	6	2

[a] [Maleic acid] = 0.1 M in water at 100 °C (substrate: catalyst = 100:1); % conversion ± 1 (TON) after 24 h.

cation is the same as that for the cation of **9b** (see above), while the ¹H spectrum shows broad singlets at δ 3.49 and 2.63 for the Me protons of the coordinated and pendant groups NMe₂, respectively (for the free ligand,[8] the Me resonance is seen at δ 2.62). Exchange behavior similar to that shown in Scheme 1 for complex **2** must occur, but the EXSY NMR spectrum was not investigated. The ¹⁹F NMR resonance at δ − 78.6 and the ν(SO) stretch at 1260 cm⁻¹ confirm the presence of a noncoordinated triflate anion.[43]

Thus, only the *P,P′,N*-coordination mode is observed for dmapcp within the chloro-Pt and chloro-Pd species, while the corresponding dmape systems generated isomeric mixtures of the neutral, dichloro-*P,P′* and cationic monochloro-*P,P′,N* species, and the latter could be isolated by abstraction of the chloride. Presumably, the difference between the dmapcp and dmape systems is dictated by the higher rigidity of the former ligand imposed by the *cyclic*-C₅H₈ ring, while the four intramolecular C−H···N interactions present in the *P,P*-bound isomer of the dmape complexes could also play a role.

The [Pd(μ-Cl)(*P,P′*-dmapm)]₂[PF₆]₂ Complex. The tridentate coordination could not be induced in the case of dmapm. Our previously reported complex PdCl₂(dmapm) (**1**),[10] which exists in CHCl₃ as an equilibrium mixture of neutral, dichloro-*P,P′*and dichloro-*P,N*-bound isomers, reacts with NH₄PF₆ in acetone to give [Pd(μ-Cl)(*P,P′*-dmapm)]₂-[PF₆]₂ (**12**).The NMR spectra show a singlet at δ_H 2.56 for the 24 equivalent NC*H*₃ protons, and an upfield δ_P singlet at −52.0 that is indicative of equivalent P-atoms involved in a four-membered metallacycle.[10] The conductivity in MeNO₂ confirms the presence of a 2:1 electrolyte.[32]

Hydration of Maleic Acid in Water. Complexes **2**, **4**, **5**, and **9** were assayed as potential catalysts for the homogeneous hydration of maleic acid, *cis*-CH(CO₂H)=CH(CO₂H), to malic acid in water at 100 °C (Chart 3), but the data (Table 6) reveal marginal activity that in the cases of **2** and **4** was comparable to that of dilute HCl. However, these cationic Pt- and Pd-dmapcp precursors (that both contain a *P,P′,N*-ligand bonding mode) give less isomerization to fumaric acid than does the HCl, and give better turn-over numbers than did Ganguly and Roundhill's [(P−P)Pd(μ-OH)]₂²⁺ complexes for the hydration of diethylmaleate in THF/H₂O (for

example, with the P−P = Ph$_2$P(CH$_2$)$_2$PPh$_2$ system, they report < 1.0 and 2.6 diethylmalate/mol catalyst after 30 h at 100 and 120 °C, respectively).[23] The nature of the species present in the aqueous solution at 100 °C in our systems is unknown, but it is worth noting that the chloro precursor **4** is more active than the iodo analogue, **5**. Itaconic acid (CH$_2$=C(CO$_2$H)CH$_2$CO$_2$H) was also tested as a substrate with **4** as catalyst, but no hydration was observed, implying that the "internal position" of the double bond as in maleic acid is not the limiting factor in the catalyzed reactions. In attempts to synthesize bridged-hydroxo complexes of the well-known type[44] used by Ganguly and Roundhill,[23] the isomeric mixture of PdCl$_2$(dmape) (**9**) was reacted with KOH in an aqueous/CH$_2$Cl$_2$ medium; however, the product precipitated with NH$_4$PF$_6$ was the remarkable dimer [PdCl(μ-N,P,O-dmapeO)]$_2$[PF$_6$]$_2$, where dmapeO is Ar$_2$P(CH$_2$)$_2$P(O)-Ar$_2$ (Ar = o-N,N-dimethylanilinyl), the monooxide of dmape.[36] Details on the characterization of this dimer, and related oxidation chemistry of these dimethylanilinyl ligands,[36] will be published elsewhere.

More generally, development of effective, transition metal catalysts for hydration of olefins remains elusive; the history of the topic can be traced through some relevant literature,[1,2,21−23,45] which includes the notable, *metal-free* phosphine systems reported recently.[22]

Conclusions

Tetra(o-anilinyl)bis(phosphine) ligands give rise to a range of fluxional coordination modes with Pt(II) and Pd(II), the nature of the fluxionality depending principally on the ligand "backbone" and to a lesser extent on the metal. Thus, dmapm shows P,P′- to P,N′-coordination exchange in chloro-Pd(II) complexes and solely P,P′-coordination within chloro-Pt(II) species;[10] dmape shows P,P′ to P,P′,N exchange in complexes of both metals; and dmapcp gives solely P,P′,N-coordination, again with both metals. In the last case, there is slow, diastereoselective exchange between bound and free anilinyl rings. The cationic Pd(II) and Pt(II) species containing P,N-bound dmapcp show marginal activity as catalytic precursors for the hydration of maleic to malic acid; the activity is comparable to that of general acid catalysis, but the selectivity (relatively less isomerization to fumaric acid) suggests a role for the metal.

Supporting Information Available: X-ray crystallographic data for the structures of **2**, **7a**, **9a**, and **11** in CIF format. The δ 2−4 range of the 2D ^{1}H EXSY spectrum of **2** (Figure S1), a PLUTO representation of the structure of **4** (Figure S2), the ^{31}P{^{1}H} spectra of **2** and **4** (Figure S3), the ^{31}P{^{1}H} NMR spectrum of an equilibirum mixture of PtCl$_2$(P,P′-dmape) (**7a**) (*) and [PtCl(P,P′,N-dmape)]Cl (**7b**) (#) (Figure S4), the van't Hoff plots for the equilibria between **7a** and **7b**, and between **9a** and **19b** (Figure S5), and a possible structure for **A** (Chart S1). This information is available free of charge from http://pubs.acs.org.

IC048639H

(43) Lawrence, G. A. *Chem. Rev.* **1986**, *86*, 17.
(44) Ruiz, J.; Vicente, C.; Marti, J. M.; Cutillas, N.; Garcia, G.; Lopez, G. *J. Organomet. Chem.* **1993**, *460*, 241. Pieri, G.; Pasquali, M.; Leoni, P.; Englert, U. *J. Organomet. Chem.* **1995**, *491*, 27.
(45) Sanford, M. S.; Groves, J. T. *Angew. Chem., Int. Ed.* **2004**, *43*, 588.